NASA Technical Memorandum 101567

ENVIRONMENTAL NOISE CHARACTERISTICS OF THE MOD5-B (3.2 MW) WIND TURBINE GENERATOR

KEVIN P. SHEPHERD
HARVEY H. HUBBARD

MARCH 1989

National Aeronautics and Space Administration

Langley Research Center
Hampton, Virginia 23665-5225

INTRODUCTION

It is desirable for developers, operators and regulators to be able to predict with confidence the noise environment around future large wind turbine generator installations. Other research programs have produced extensive acoustic measurements and observations for horizontal axis wind turbines (both upwind and downwind configurations) for a wide range of sizes (power ratings) and operating conditions (see Refs. 1-8). The results to date have provided a basis for development of interim environmental noise impact criteria for siting and operations of wind power stations as well as a data bank for validation of noise prediction models.

The present study provides basic acoustic data for the MOD5-B machine and extends the previously available data base with results for a machine which incorporates advanced technology features such as variable rpm, trailing edge tabs and vortex generators.

This effort is part of the Department of Energy Wind Energy Program managed by the Solar Energy Research Institute. Data were obtained with the assistance and cooperation of the Boeing Company personnel at the site.

APPARATUS AND METHODS

Description of Machine

The MOD5-B machine has a two-bladed 97.6 m diameter rotor mounted on a 61 m high, 3 m diameter circular cross section tower (figure 1). It is an upwind machine with a maximum power rating of 3.2 MW and an operational range of wind velocities from 5.4 to 26.8 m/s. The outer 16.8 m of each blade is movable in pitch and is adjusted by a hydraulic control system. A variable rpm feature is included. The machine operates at about 13 rpm for wind speeds from 5.4 m/s (cuts in or starts operating) to about 8.1 m/s. For wind speeds from 8.1 to about 10.7 m/s the rpm varies up to 17.3 rpm and it remains

at 17.3 rpm at wind speeds up to cut-out at 26.8 m/s where it stops operating. Rated wind speed at the hub is 12.5 m/s.

Vortex generators are installed on the suction side of the blade along the 10 percent chord line and for the outboard 40 m of the blade. Flat plates varying in length from 2.5 to 8 cm and in height from 0.6 to 2 cm were installed in pairs at 20° angles to the alignment line. Spacing within pairs varied from 10 to 15 cm and between pairs from 20 to 30 cm.

A streamwise trailing edge tab extended the length of the blade and its extension was 2-4% of the chord length. The outboard portions of the tab were formed by an aft extension of the airfoil suction surface skin beyond its normal trailing edge termination.

During the tests wind speed, wind direction, output power and generator rpm were recorded in addition to the acoustic data.

Description of the Site

The wind turbine site at which acoustic data were obtained is in the Kahuku Point region of Oahu, HI (figure 2). The wind turbine installation is about 4 km from the northeast coast of Oahu and is located on a ridge at an elevation of about 125 m above sea level. Ground elevations as a function of distance out to 500 m from the machine are shown in the inset of figure 2, for the two different wind directions for which data were obtained. Terrain upwind of the machine in both directions is seen to slope rather steeply upward to the edge of the flat area at the site. Vegetation consisted of thick grass; and only a sparse stand of bushes and trees.

Prevailing winds came from the east to northeast and blew steadily in the range 6.3 to 13.4 m/s during the tests. Wind speed values are 30 second averages derived from nacelle anemometer readings, or are computed values based on a knowledge of the generated power.

Noise Measurements and Analyses

Noise measurements were made with commercially available battery powered instrumentation. One-half inch diameter condenser microphones with a useable frequency range 3-20,000 Hz were used with a four channel FM tape recorder having a useful dynamic range of 40 dB in the frequency range of 0-15,000 Hz.

Acoustic data were obtained for distances from about 30 to 330 m, at various azimuth angles around the machine and for daytime and nighttime operations over a range of power outputs. All acoustic data were recorded on magnetic tape for later analyses. Spectral data were obtained with the aid of conventional one-third octave and narrow band ($\Delta f = 0.05$ Hz) analyzers.

To minimize the detrimental effects of wind noise, polyurethane foam microphone wind screens were used and microphones were placed at the ground surface, where wind velocities were relatively low.

RESULTS AND DISCUSSION

Noise data presented herein were obtained from FM tape recordings and are in the form of directivity patterns, one-third octave band frequency spectra, and narrow band frequency spectra.

Directivity Patterns

Figure 3 presents dBA-levels which are a frequently employed measure of community acceptance. These data were obtained from analyses of data recorded during the MOD5-B tests and are categorized as high power (1566-3100 kW, 17.10-17.48 rpm) and low power (300-1166 kW, 13.7-13.85 rpm) for comparison. Data are adjusted by the inverse distance law, to a given reference distance of 244 m (2.5 diam.). The increased power output/rpm condition results in a 4-6 dB increase in the dBA levels. Note that the radiation patterns are

not highly directional but that consistently higher "A"-levels are measured upwind than downwind.

Broadband Noise Components

Near Field Measurements - Figure 4 presents one-third octave band spectra obtained for both low and high power operating conditions of the machine at a distance of 68 m in the upwind quadrant. It can be seen that the higher noise levels are associated with the higher power output/wind speed conditions. At the higher wind speed, the rotor turns at a higher rpm than at the lower wind speed, with a resulting higher tip speed. The differences in tip speed are believed to largely account for the sound pressure level differences of the figure. The blocked in symbols of the figure identify data recorded after sunset. Note that no clear trend is indicated by the daytime-nighttime results in contrast to those of Ref. 8 which showed consistently lower levels at night than during the day.

Far Field Measurements - Experimental data are presented in figures 5 and 6 for far field conditions. Data measured at the indicated distances are normalized by using the inverse distance law and a reference distance of 244 m (2.5 diameters) for comparison. In figure 5, on-axis data both upwind and downwind and for both high and low power (rpm) conditions are presented. Sound pressure levels are seen to be highest at the lowest frequencies and generally decrease as the frequency increases. Note that the sound pressure levels for the high power conditions are about 5-10 dB higher than those for the low power conditions, due mainly to the higher tip speeds. Similar data are shown in figure 6 for the crosswind (in-plane) orientation. Trends in the data of figure 6 are the same as those of figure 5 but the sound pressure levels are generally lower.

Note that the overall variability in the data of figures 5 (a) and (b) is about $\pm$ 5 dB. Note also that in each case the upwind spectra (observer azimuth angle $\approx 0^{o}$) group closely together at the higher frequencies and have higher levels than the corresponding down wind

spectra (observer azimuth angle $\approx 180^{o}$). These results are consistent with the data of figure 3.

The blocked in symbols of figures 5 and 6 are coded to indicate those data recorded after sunset. As in figure 4 and Ref. 8 there is no clear trend toward lower levels at night.

Comparisons with Predictions - Extensive research has resulted in the identification of the main broadband noise sources for wind turbine rotors (Ref. 9). These are aerodynamic loading fluctuations due to inflow turbulence interacting with the rotating blades; the turbulent boundary layer flow over the airfoil surface interacting with the blade trailing edge; and vortex shedding due to trailing edge bluntness. A method for predicting the overall broadband noise spectra from the above components based partly on empirical considerations is presented in Ref. 9 and is used for the broadband noise predictions of figure 7.

Figure 7 presents example one-third octave band spectra for both low output power and high output power conditions. Each shaded region is a composite of five or six different spectra measured on the axis both upwind and downwind, and adjusted to a reference distance of 244 m (2.5 times the rotor diameter). Shown also are predicted curves based on the method of Ref. 9.

Figure 7(a) relates to the low output power conditions of the MOD5-B machine, for which the rotor is turning at about 13.75 rpm. Note that the measured spectra peak at frequencies below 30 Hz and then generally decrease in level as frequency increases. Similar results are given in figure 7(b) which relates to the high power operating conditions of the MOD5-B machine for which the rotor turns at about 17.3 rpm. Note that the increase in rotor rpm results in increases of 5-10 dB in both the measured and calculated sound pressure levels, compared to those of figure 7(a).

The predicted curves are seen to follow the general trends of the data. However, they tend to underestimate the band levels in the 200 Hz - 2000 Hz frequency range where the turbulent boundary layer-trailing edge interaction noise component is expected to be significant. These differences are not understood but may arise because the effects of trailing edge tabs have not been properly accounted for in the predictions. Possible vortex generator effects are expected to be minimal, based on the data of Ref. 5.

Comparisons with other Large Machines - Shown in figure 8 are broadband spectral data for the high power condition of the MOD5-B machine compared with similar on-axis data for the Boeing MOD-2, Westinghouse WWG-0600 and Hamilton Standard WTS-4 machines at a reference distance of 2.5 diameters. Listed on the figure are output power, tip speed and rotor diameter for each machine. The WTS-4 machine generates the highest levels, probably because of its relatively higher tip speed and the existence of tower-wake blade interaction noises at low frequencies (see Ref. 7). The MOD-2 machine has the lowest tip speed and no tower-wake noise; and its noise levels are generally lower than those of the others (Ref. 5). The MOD5-B and unpublished WWG-0600 noise spectra fall generally between those of the other two.

Low Frequency Rotational Components

Example Spectra - The nature of the low frequency noise components for the MOD5-B machine is shown in the measured narrow band (Δf = 0.05 Hz) spectra of figure 9. The top portion of the figure shows a spectrum measured at ground level 68 m from the rotor hub and upwind of the plane of rotation. About a dozen well defined low frequency components are evident. These are identified as rotational harmonics which are integer multiples of the blade passage frequency (0.58 Hz).

Similar peaks are also present in the far field spectrum of figure 9, which was measured downwind at a distance of 118 m, but they are not so easily identified. Rotational noise

harmonic components are not normally present for an upwind configuration of machine for which there is no tower-wake blade interaction noise. Careful evaluations of the recorded time histories suggest that the rotational harmonic levels do not vary appreciably with time and thus probably result from relatively stable flow conditions. There is thus a very low probability that atmospheric turbulence is the cause of this enhancement of the rotational noise components. A more probable reason for the enhancements of the rotational harmonics for this machine is believed to be an unusual inflow wind profile to the rotor due to terrain effects. Reference 10 contains a convenient method for predicting the rotational harmonic levels of wind turbines, provided the geometry and operating conditions of the rotor are known. It incorporates unsteady aerodynamic blade forces and is based on previous developments by Sears (Ref. 11) and Lowson (Ref. 12). The role of low frequency noise components is illustrated in figures 10-14 as derived from a series of calculations by the method of Ref. 10.

Comparisons of Measurements and Predictions - Figure 10 shows several different inflow wind profiles that were evaluated. Profile A corresponds to that which is believed to exist over smooth ground and is described by the 1/7 power law. Likewise profiles B and C are believed to characterize the inflow over rough ground and over very rough terrain respectively. Profiles D, E, F and G were arbitrarily assumed in an attempt to represent progressive shadowing of the bottom of the rotor disk as shown in the sketches of the figure.

The results of calculations using profiles A, B and C are shown in figure 11 and are compared with two sets of measured data. It can be seen that the use of the above wind profiles result in calculated sound pressure level values that are much lower than the measured values. Other assumed profiles (E, F and G) were also used as inputs in an attempt to achieve better agreement. Results of these latter calculations are presented in figure 12 for an assumed shadow angle (see figure 10) of 45^{o}. It can be seen that the

higher calculated sound pressure level values are associated with the higher values of wind speed deficit. Individual points are connected by straight lines for identification in figure 12 and the useful concept of spectrum envelope is defined for use in figures 13 and 14.

In figure 13 the experimental data are compared with the spectrum envelopes computed for profiles E, F and G respectively. The experimental data seem to scatter around the computed spectrum envelop for profile F which involved a wind speed deficit of 3.6 m/s over the bottom portion of the rotor disk subtended by a 45^{o} shadow angle.

Both the shadow angle and the wind speed deficit are judged to be significant variables, however no pertinent experimental wind speed data are available as inputs. Thus, there is at present no unique solution. In order to demonstrate the sensitivity of the calculations to various assumed values of wind speed deficit and shadow angle the calculated results of figure 14 are presented. Note that the calculated spectrum envelope levels are about 6 dB higher for either a doubling of the wind speed deficit for a given shadow angle or a halving of the shadow angle for a given wind speed deficit.

CONCLUDING REMARKS

One-third octave band spectra for the MOD5-B machine have the highest sound pressure levels at the lowest frequencies and these levels generally reduce as frequency increases. These spectra generally follow the shapes of comparable spectra for other large machines. Several on-axis measurements are within $\pm$ 5 dB for both upwind and downwind locations and for both daytime and nighttime operations when adjusted to the same reference distance. Cross wind spectra have about the same range of variability and have lower levels than on-axis spectra. An increase in rpm from 13.75 to 17.3 results in a 5-10 dB increase in both the measured and predicted levels. Predicted broadband spectra follow the general trends of the data but tend to underestimate the levels in the frequency

range where the turbulent boundary layer - trailing edge interaction noise is expected to be significant.

The sound pressure level values of the rotational harmonics (discrete frequencies at integer multiples of the blade passage frequencies) were higher than anticipated. This enhancement of the rotational harmonics is believed due to shadowing of a portion of the rotor disk because of effects of terrain upstream of the rotor. Example calculations show sensitivity to both the shadow angle of the rotor disk and the associated wind speed deficit.

REFERENCES

1. Kelly, N. D., McKenna, H. E., Hemphill, R. R., Etter, C. L., Garrelts, R. L. and Linn, N. C.: Acoustic Noise Associated with the MOD-1 Wind Turbine: Its Source, Impact and Control. SERI TR-635-1166, February 1985.

2. Hubbard, Harvey H., Grosveld, F. W. and Shepherd, Kevin P.: Noise Characteristics of Large Wind Turbine Generators. Noise Control Engineering Journal, Vol. 21, No. 1, pp. 21-29, 1983.

3. Kelley, N. D., McKenna, H. E., Jacobs, E. W., Hemphill, R. R. and Birkenheur, N. R.: The MOD-2 Wind Turbine: Volume 1, Aeroacoustic Noise Sources, Emissions and Potential Impact. SERI TR217-3036, April 1987.

4. Ljungren, Sten: A Preliminary Assessment of Environmental Noise from Large WECS, Based on Experiences from Swedish Prototypes. FFA-TN-1984-48, 1984.

5. Hubbard, Harvey H. and Shepherd, Kevin P.: The Effects of Blade Mounted Vortex Generators on the Noise from a MOD-2 Wind Turbine Generator. NASA CR172292, February 1984.

6. Hubbard, Harvey H. and Shepherd, Kevin P.: Noise Measurements for Single and Multiple Operation of 50 kw Wind Turbine Generators. NASA CR-166052, December 1952.

7. Shepherd, Kevin P. and Hubbard, Harvey H.: Measurements and Observations of Noise from a 4.2 Megawatt (WTS-4) Wind Turbine Generator. NASA CR-166124, May 1983.

8. Shepherd, Kevin P., Willshire, William L., Jr. and Hubbard, Harvey H.: Comparisons of Measured and Calculated Sound Pressure Levels Around a Large Horizontal Axis Wind Turbine Generator. NASA TM-100634, 1988.

9. Grosveld, F. W.: Prediction of Broadband Noise from Large Horizontal Axis Wind Turbines. AIAA Journal of Propulsion and Power. Vol. 1, No. 4, July-August 1985.

10. Viterna, Larry A.: The NASA-LERC Wind Turbine Noise Prediction Code. NASA CP-2185, February 1981.

11. Sears, William R.: Some Aspects of Non-Stationary Airfoil Theory and Its Practical Applications. J. Aeron. Sci., 83, 1941.

12. Lowson, M. V.: Theoretical Analysis of Compressor Noise. J. Acous. Soc. of Amer., 47, 1 (Part 2) pp. 371-385, 1970.

ORIGINAL PAGE
BLACK AND WHITE PHOTOGRAPH

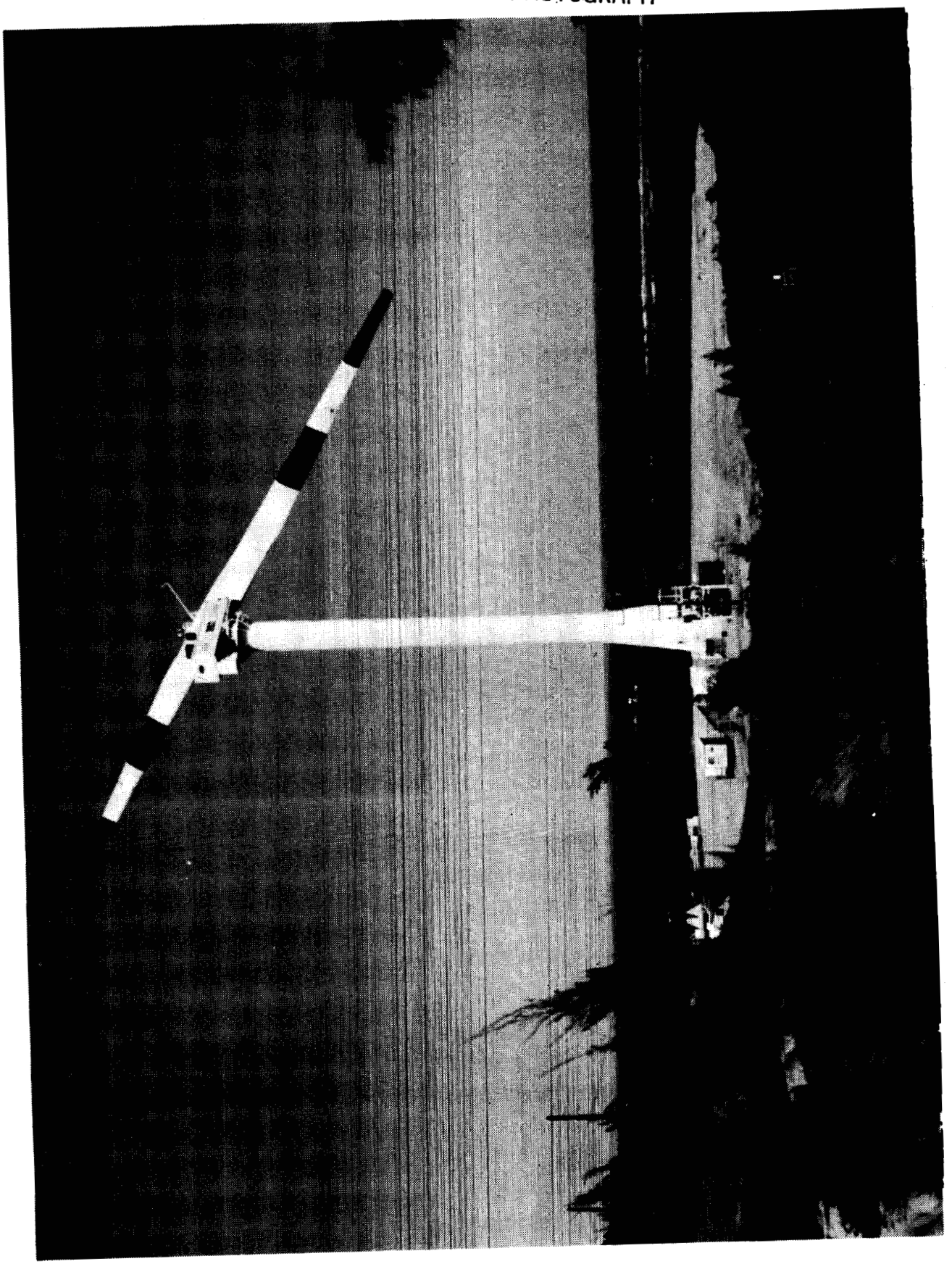

Figure 1. - MOD5-B Wind Turbine Generator.

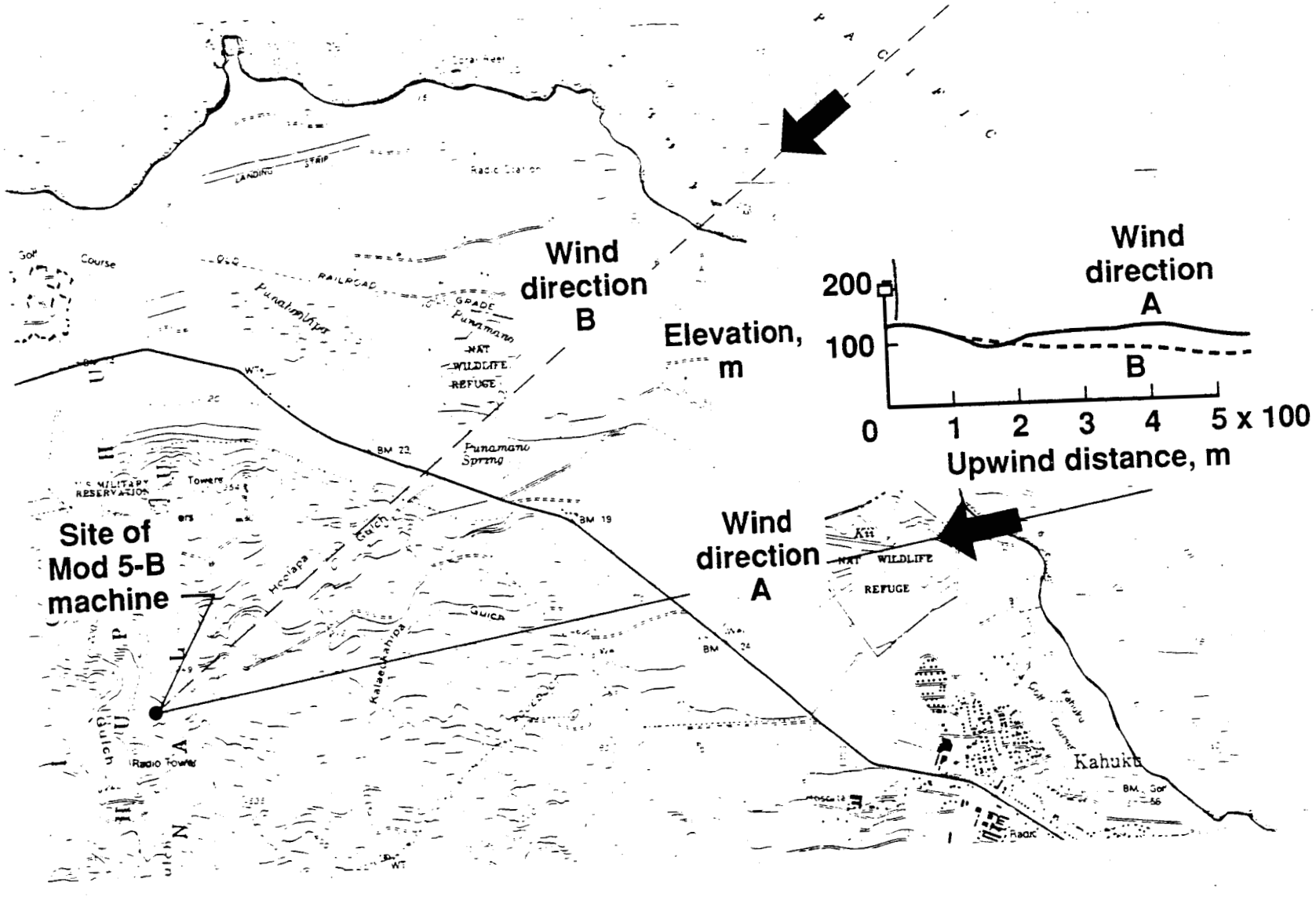

Figure 2. - Location of MOD5-B test site.

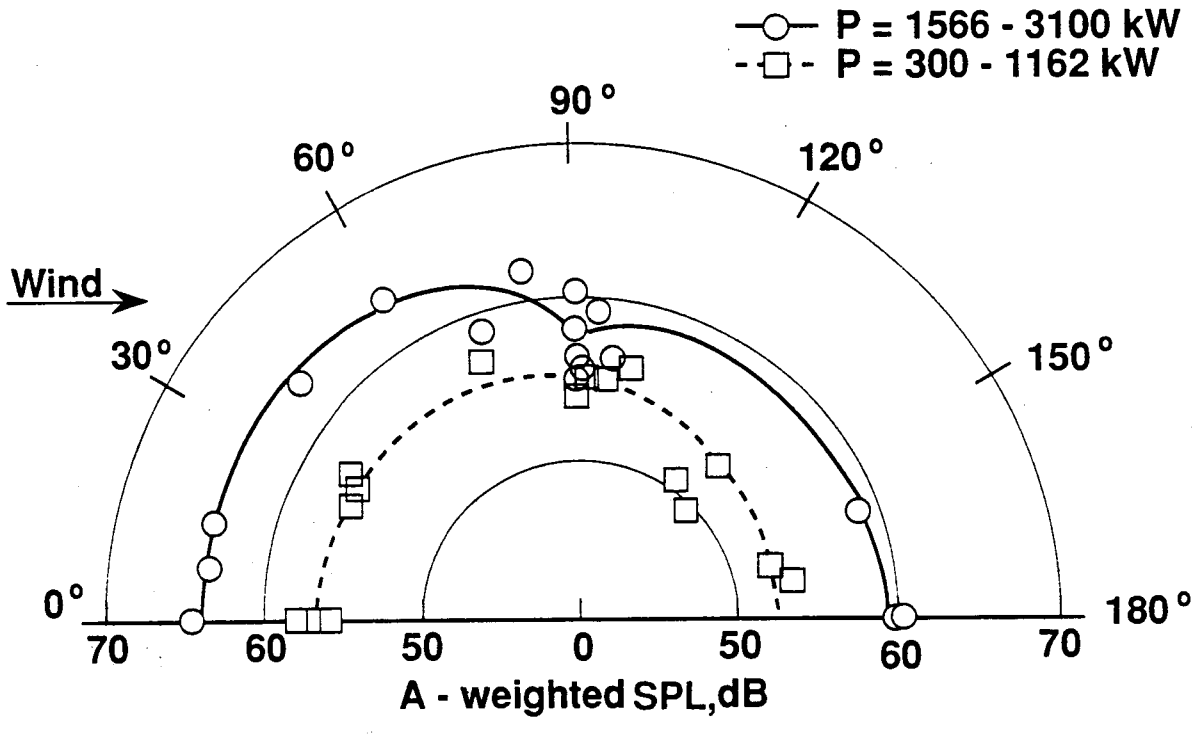

Figure 3. - "A" - weighted sound pressure level directivity patterns for both low and high power operating conditions of the MOD5-B machine. All data are adjusted to a reference distance of 2.5 diameters.

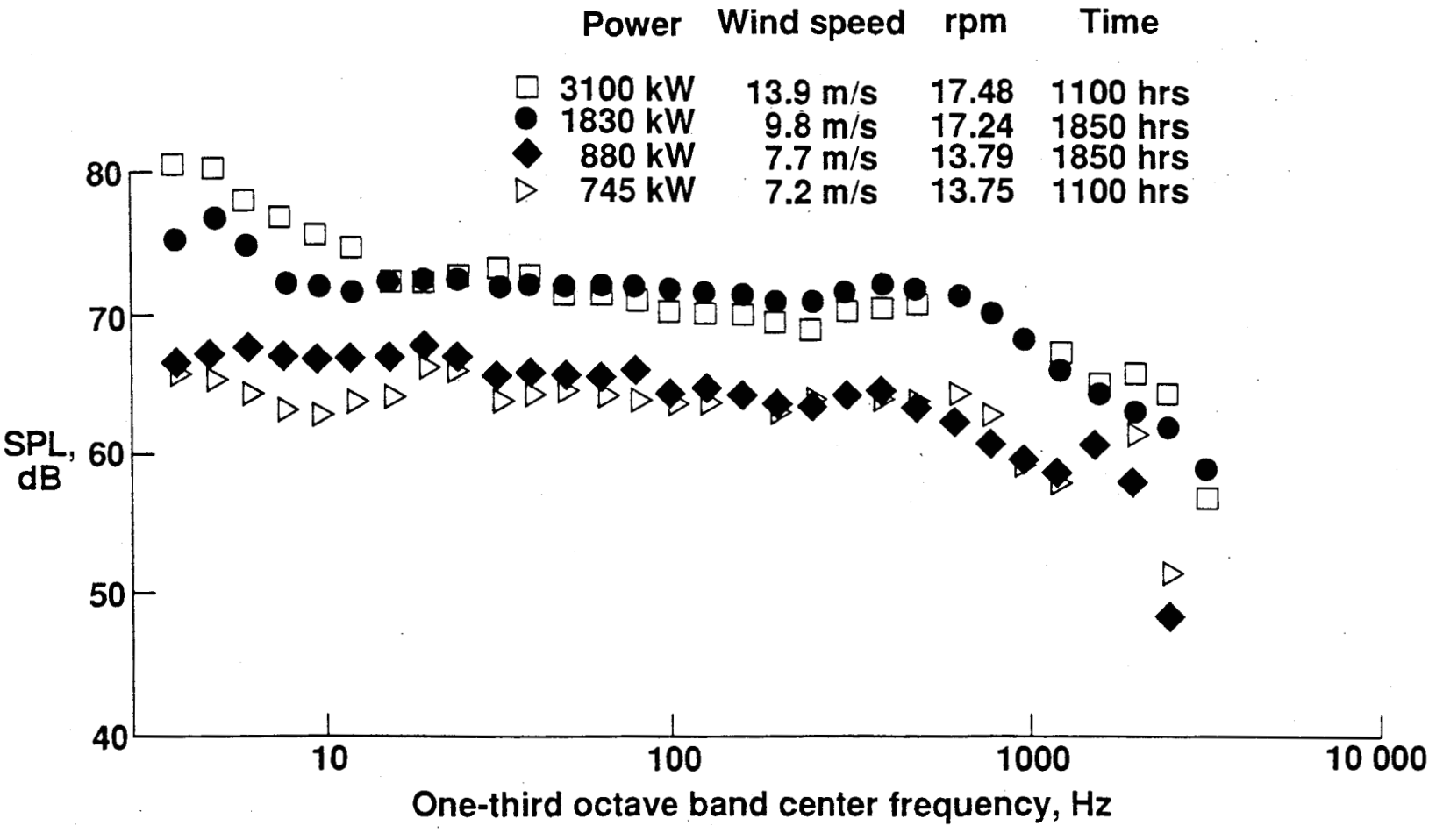

Figure 4. - Near field broad band noise spectra for the MOD5-B machine at two different operating conditions. d = 68 m.

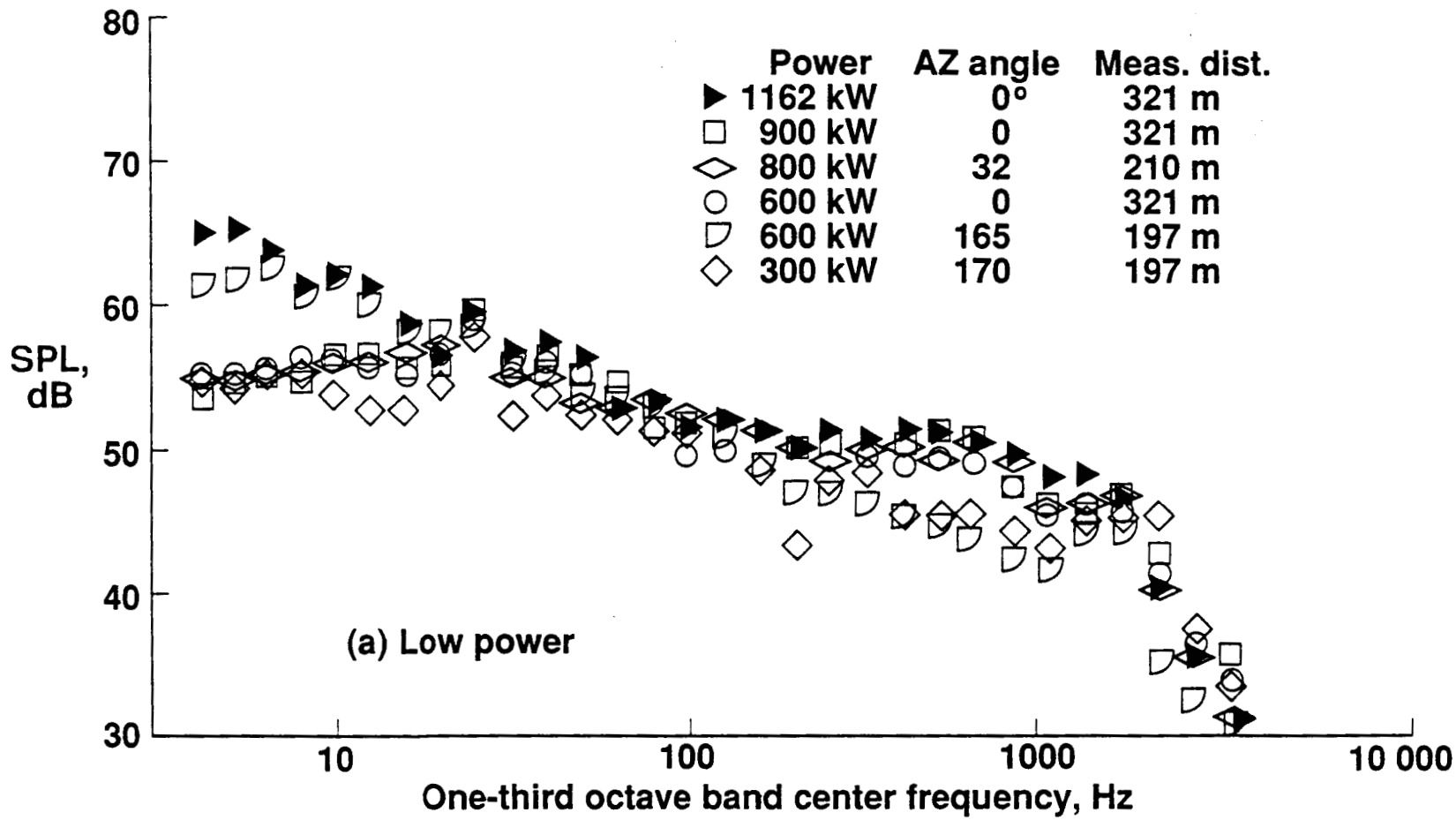

Figure 5. - On-axis measured one-third octave band noise spectra for both low and high power operating conditions of the MOD5-B machine, adjusted to a reference distance of 2.5 diameters.

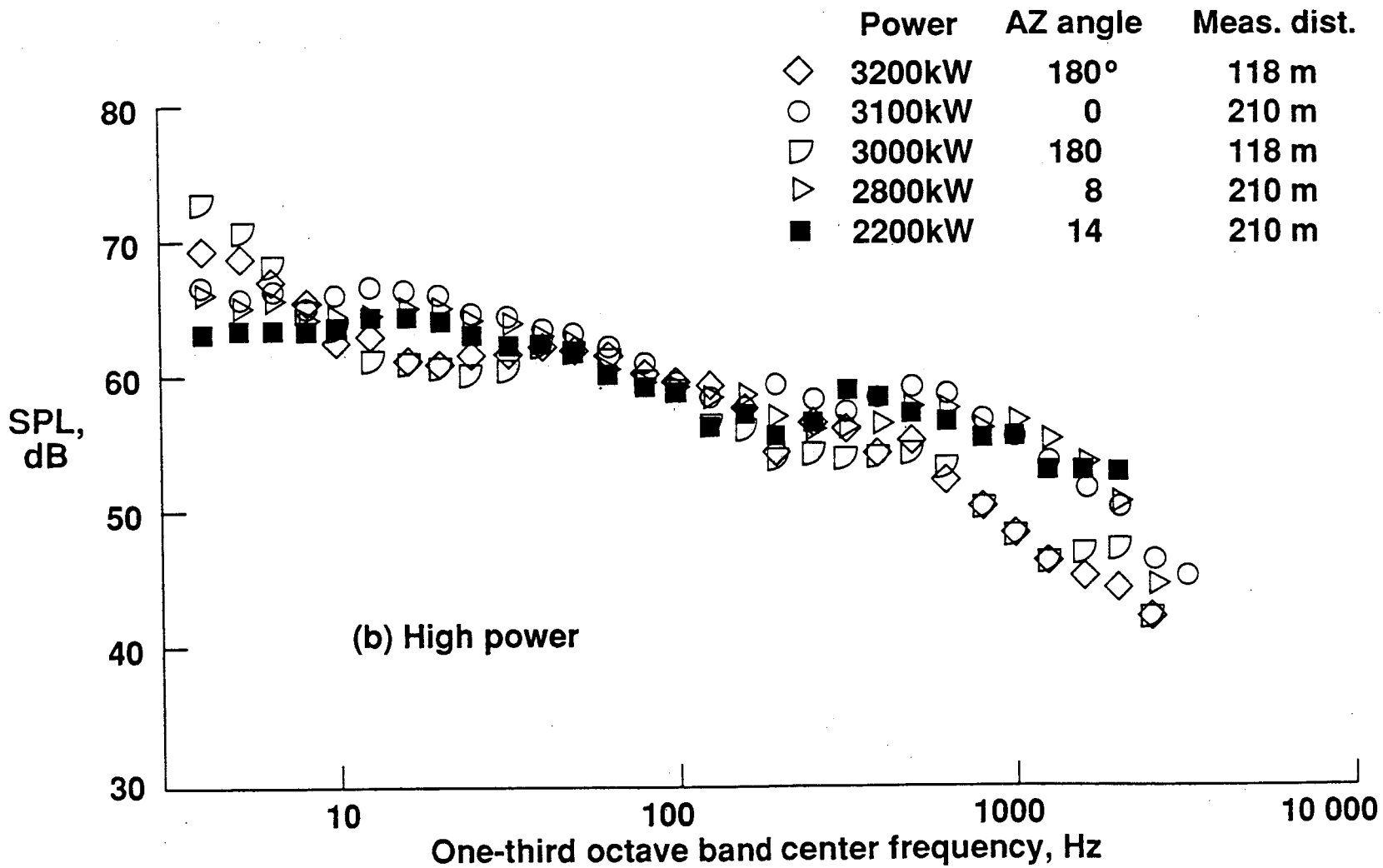

Figure 5. - (Concl.)

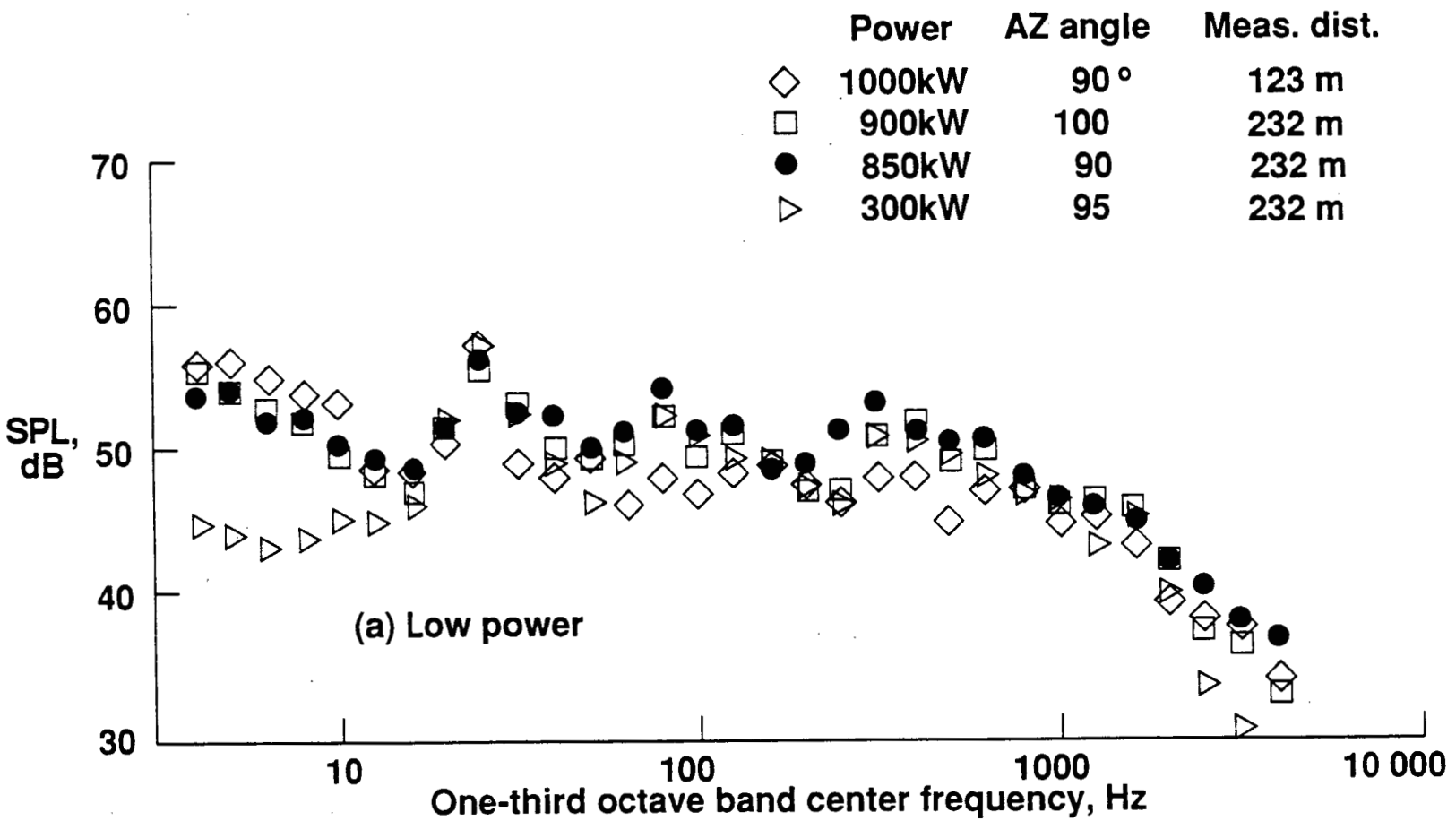

Figure 6. - In-plane measurements of one-third octave band noise spectra for the MOD5-B machine at both low and high power operating conditions, adjusted to a reference distance of 2.5 diameters.

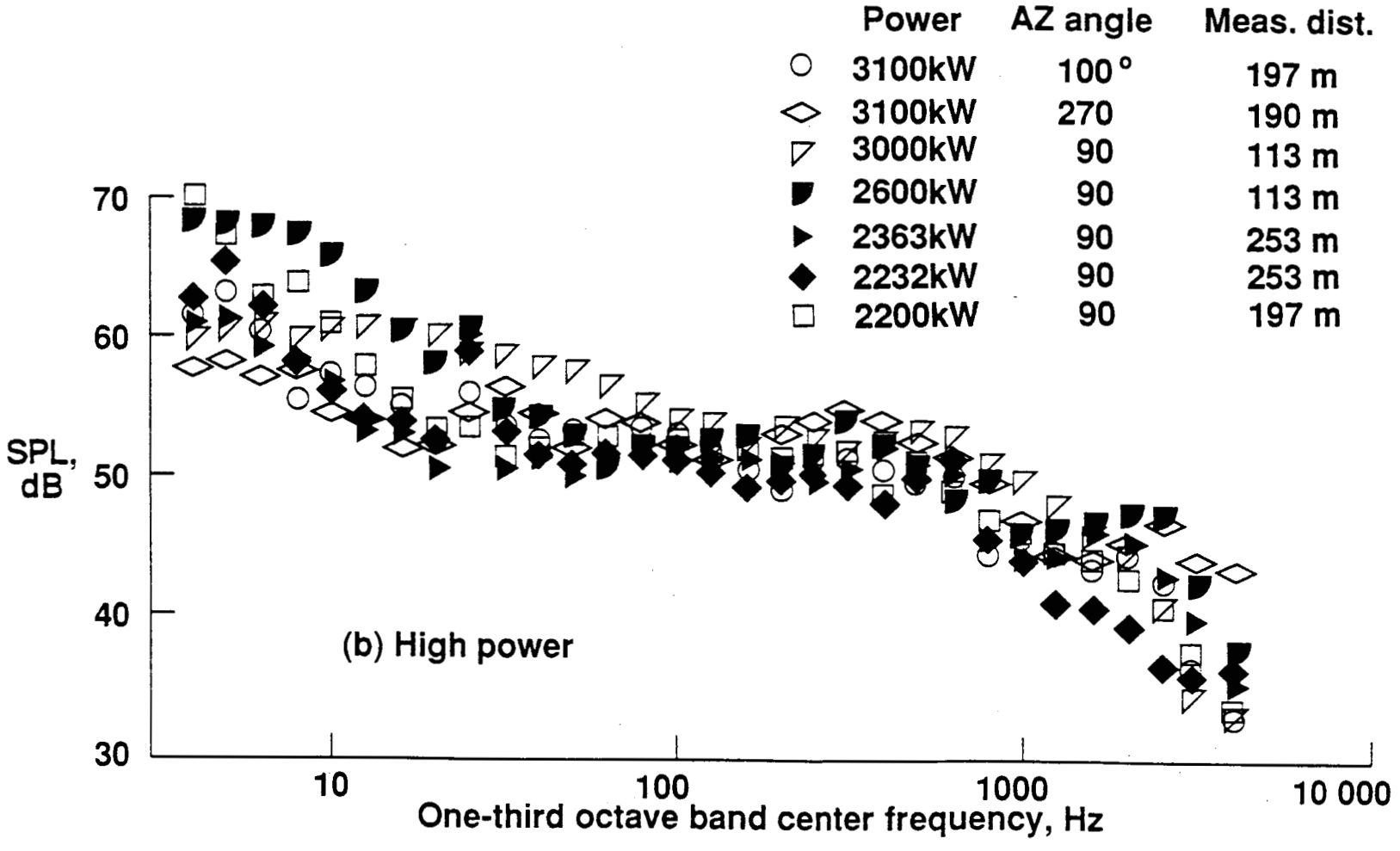

Figure 6. - (Concl.)

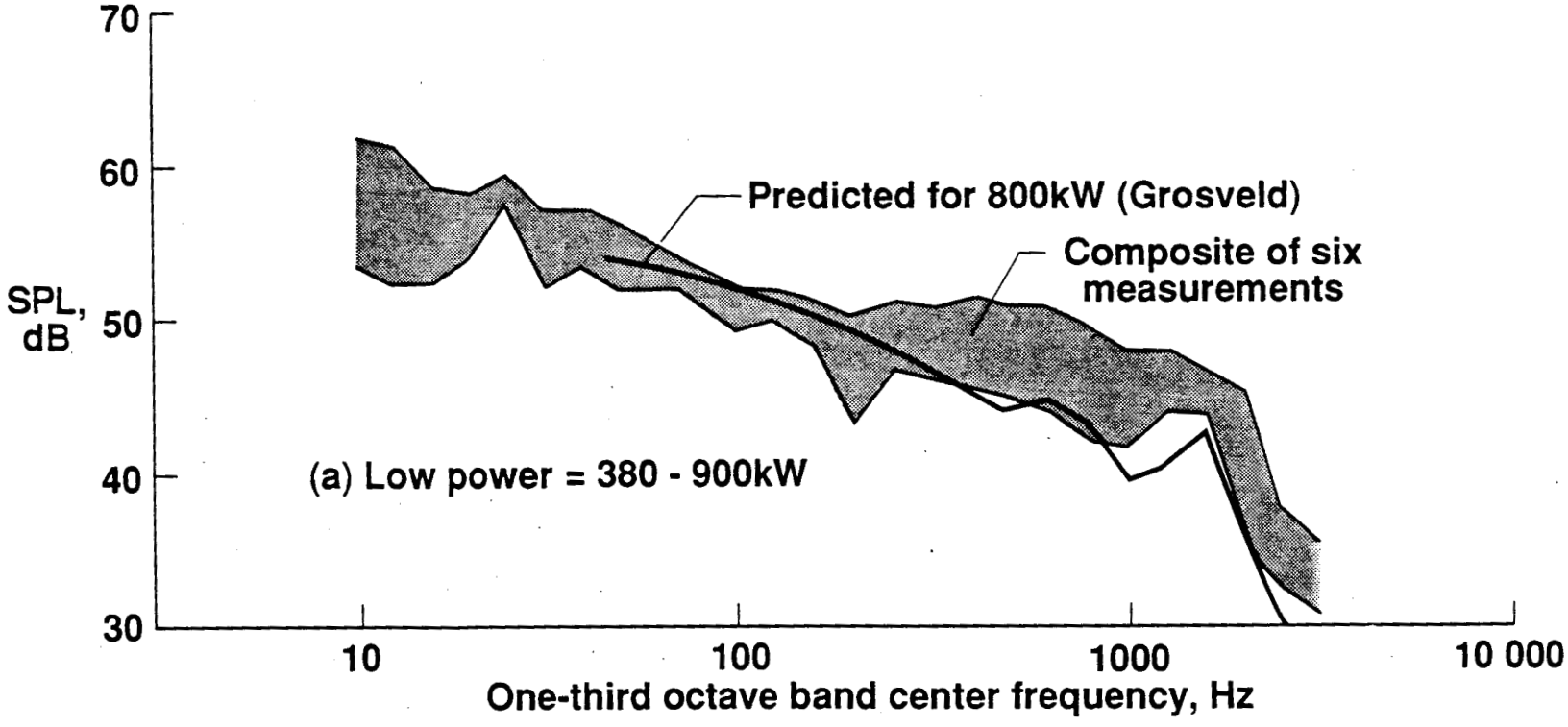

Figure 7. - Comparison of calculated and measured one-third octave band noise spectra for both low and high power operating conditions of the MOD5-B machine, on-axis, at a reference distance of 2.5 diameters.

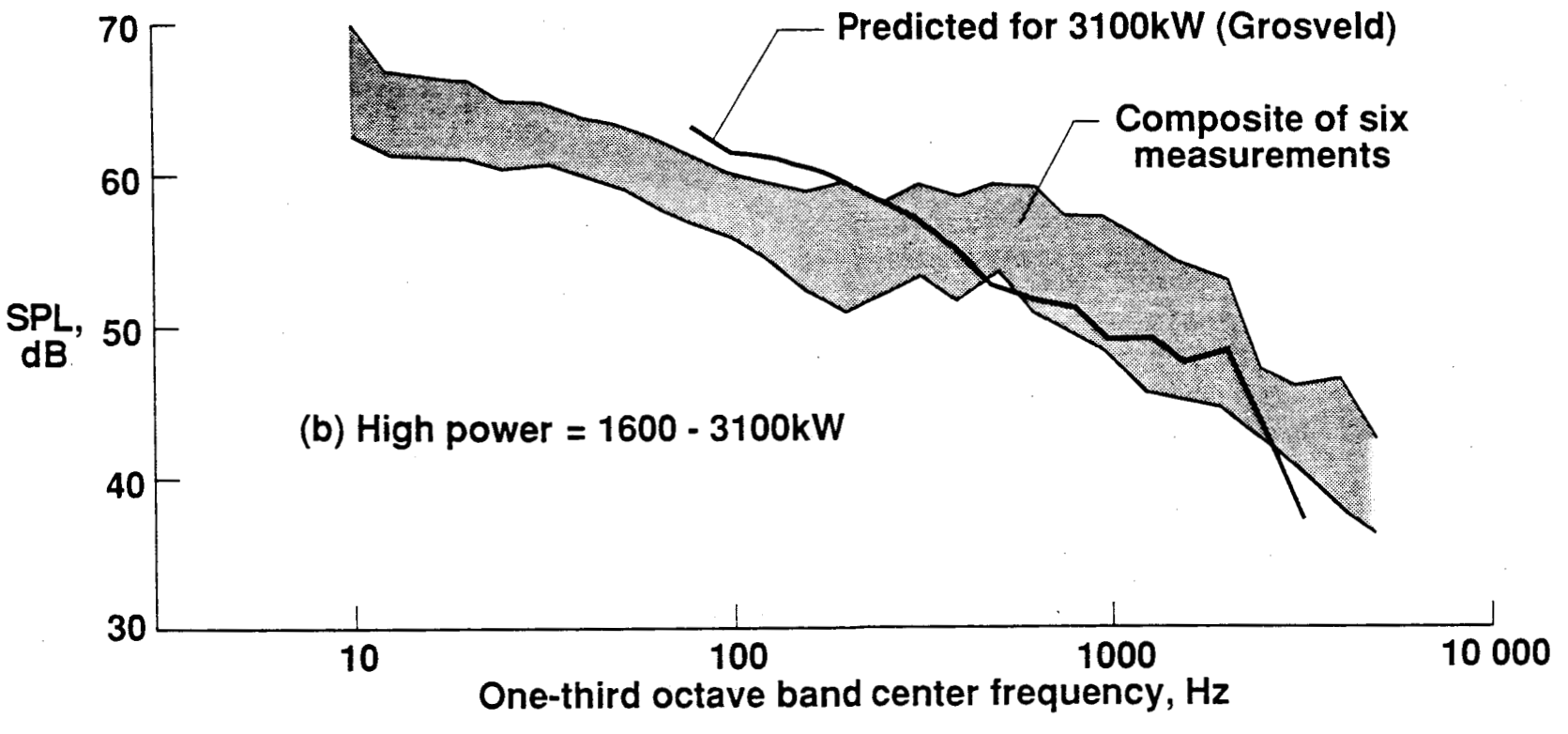

Figure 7. - (Concl.)

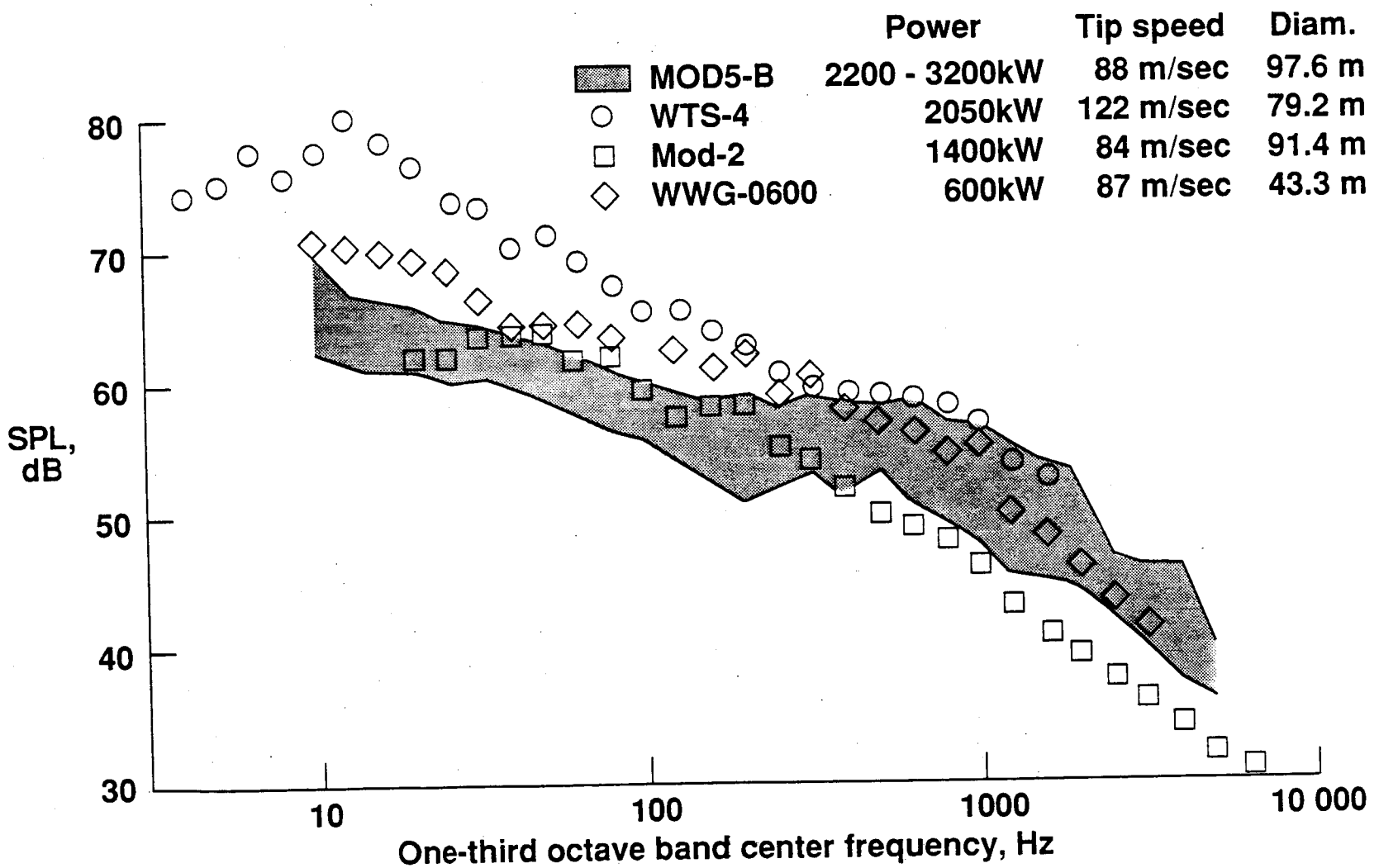

Figure 8. - Comparisons of measured one-third octave band noise spectra of the MOD5-B machine with those of other large machines at high power conditions, on-axis, at a distance of 2.5 diameters.

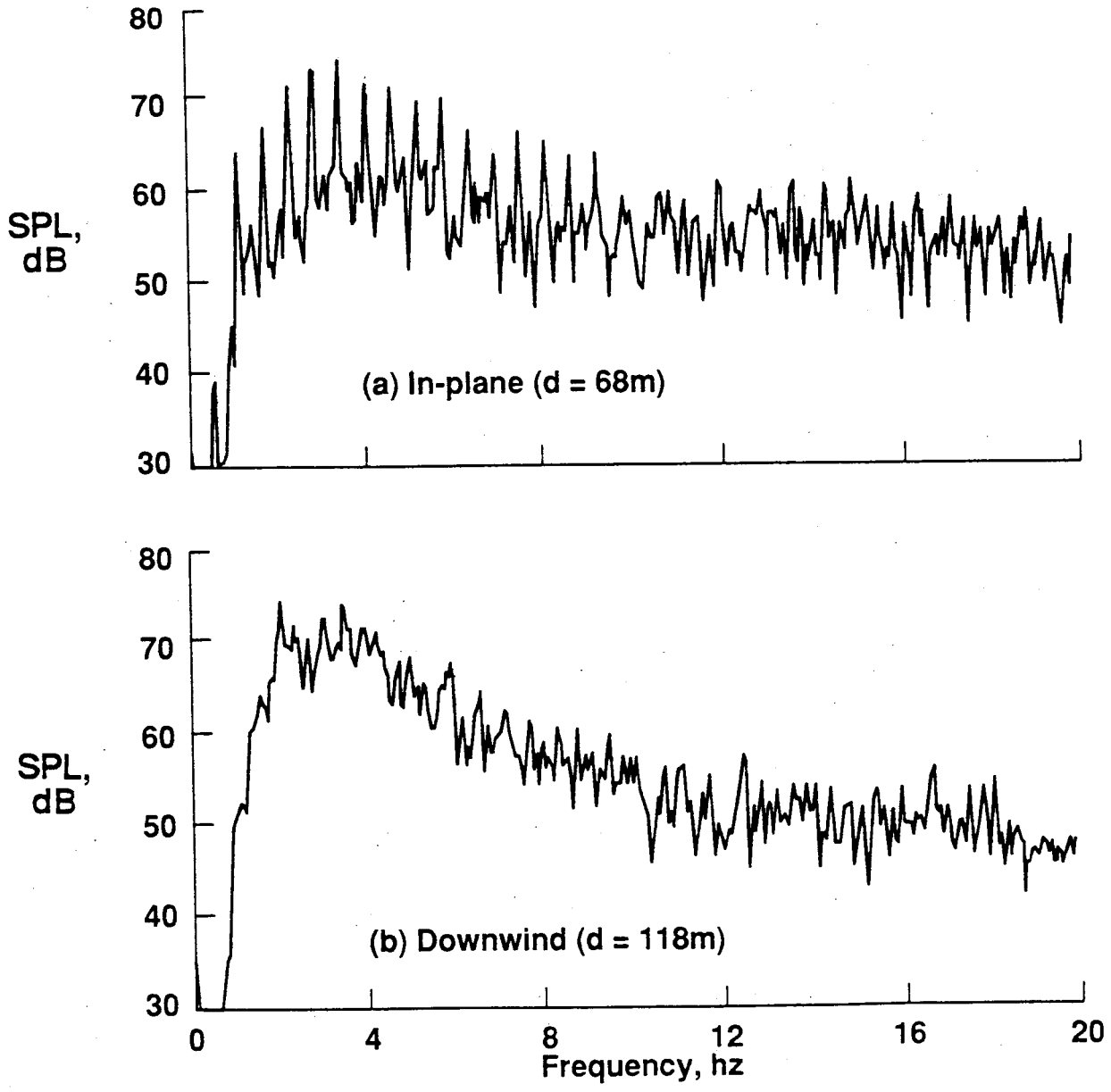

Figure 9. - Narrow band (Δf = 0.05 Hz) noise spectra for the MOD5-B machine.

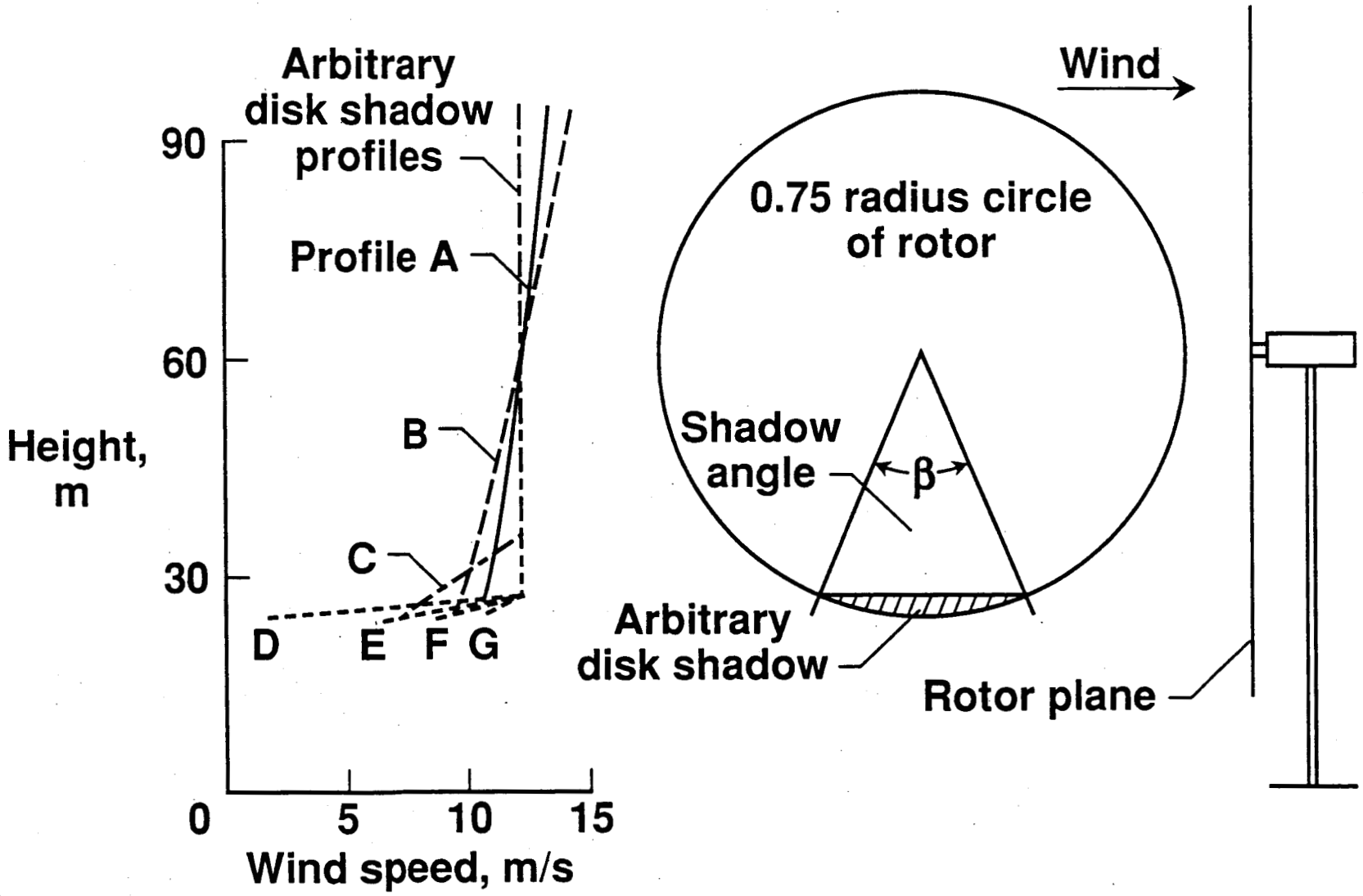

Figure 10. - Assumed wind profiles for calculating rotational harmonic sound pressure levels for the rated power condition of the MOD5-B machine, by the method of Ref. 10.

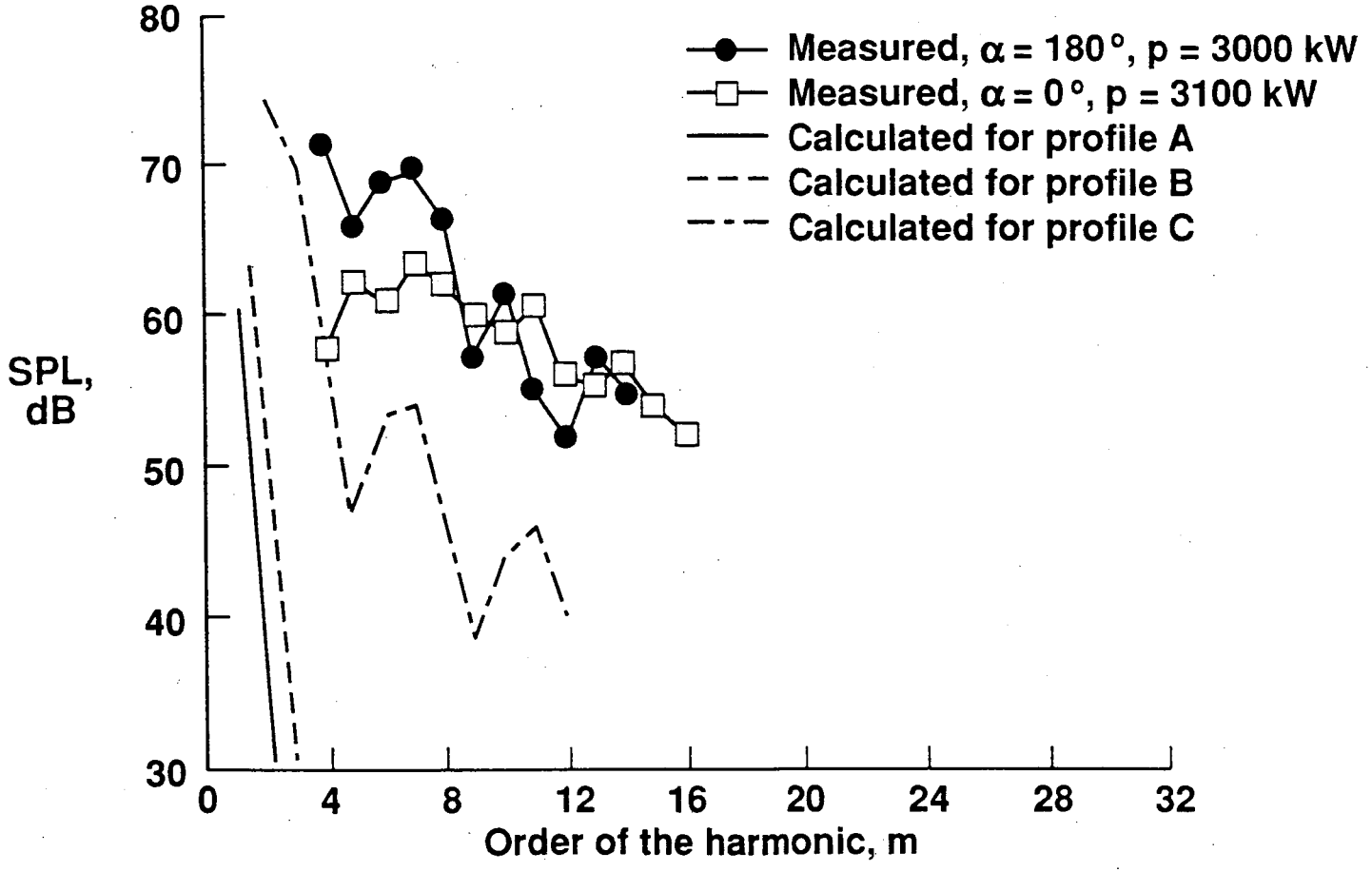

Figure 11. - Comparisons of measured and calculated rotational harmonic levels for assumed wind profiles A, B and C for the MOD5-B machine at rated power.

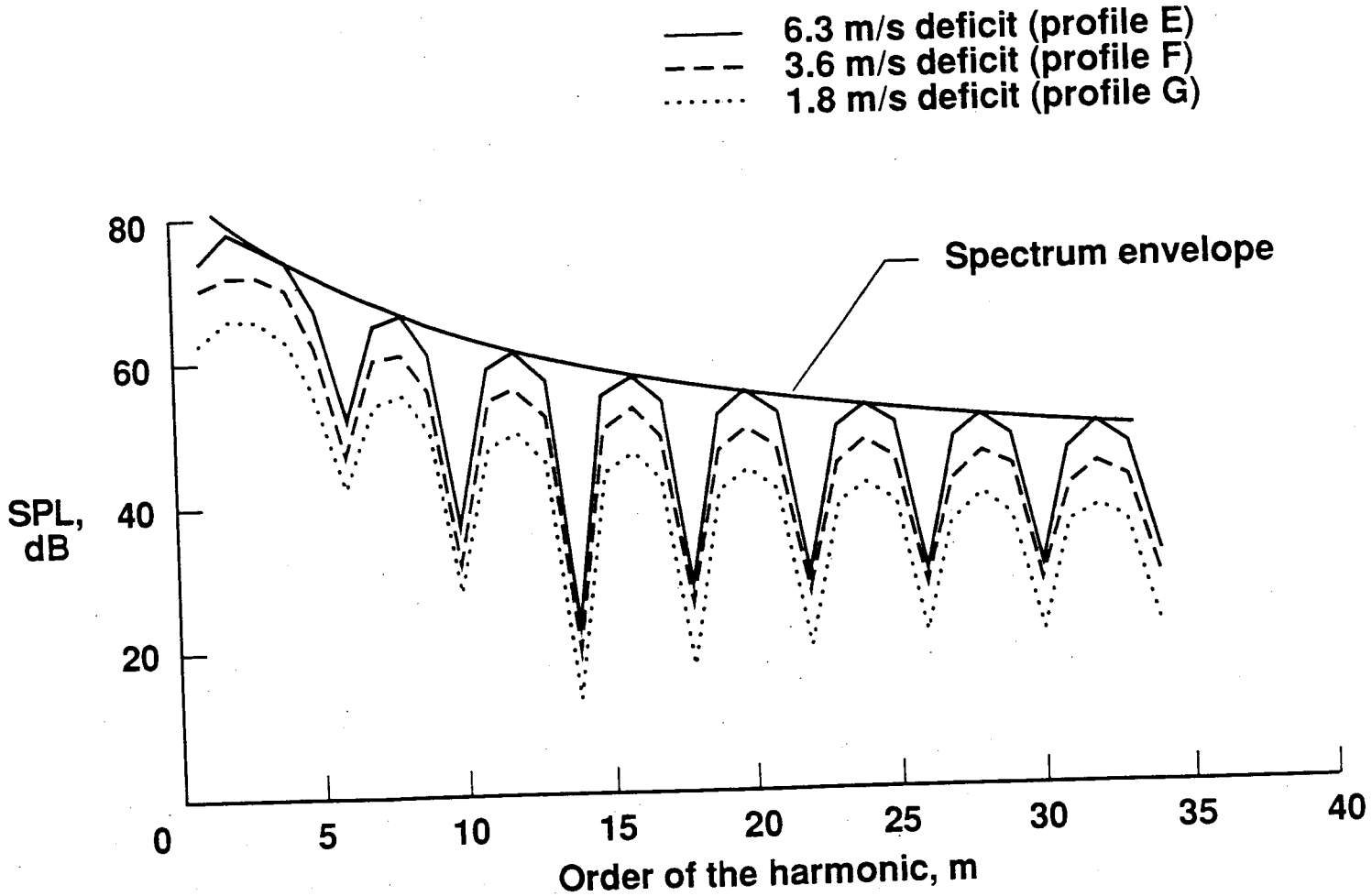

Figure 12. - Calculated levels of rotational harmonics of the MOD5-B machine due to rotor disk shadowing. ß = 45°, P = 3200 kW, V = 12.5 m/s.

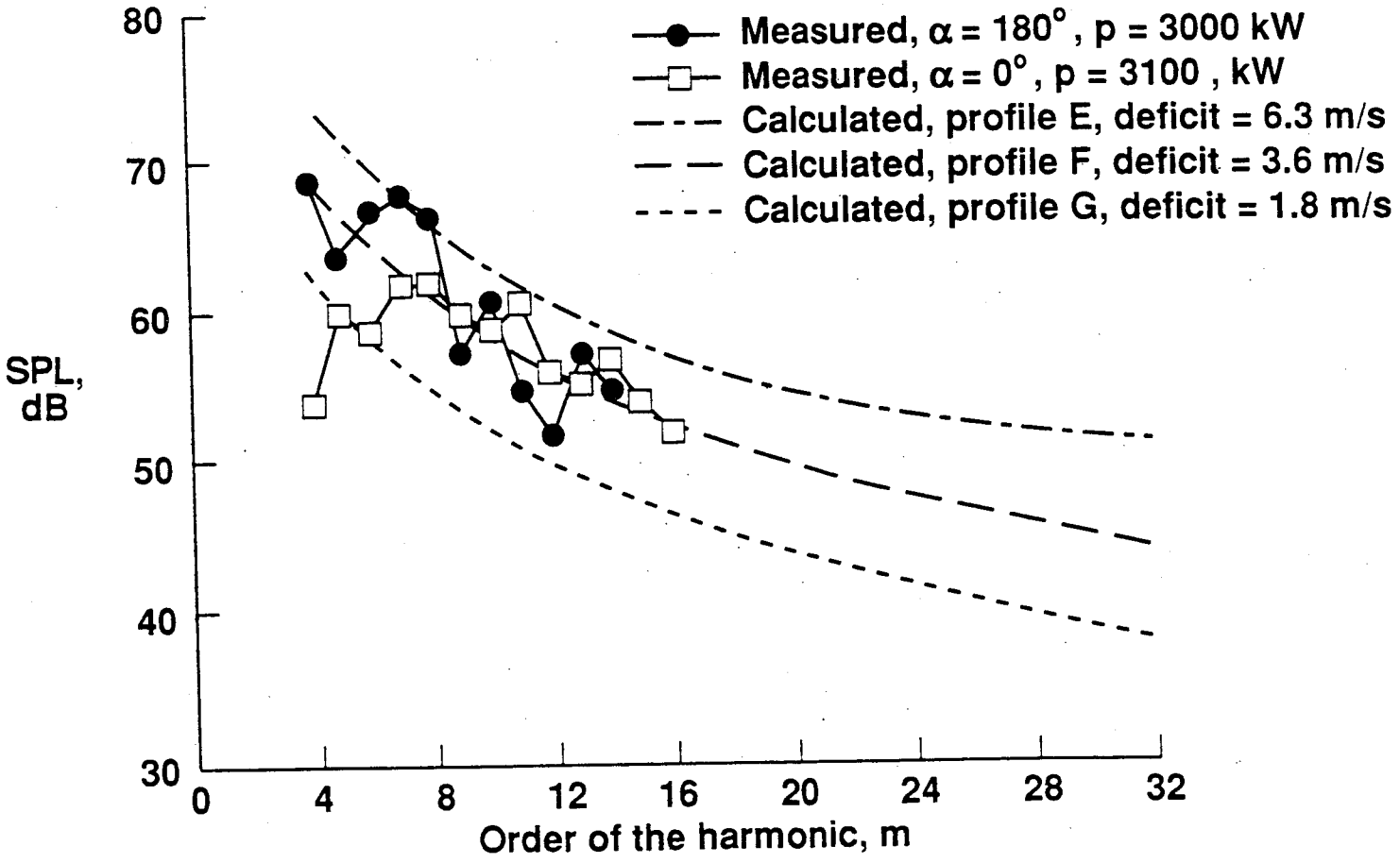

Figure 13. - Comparisons of measured and calculated rotational harmonic levels for assumed wind profiles E, F and G for the MOD5-B machine at rated power. ß = 45°.

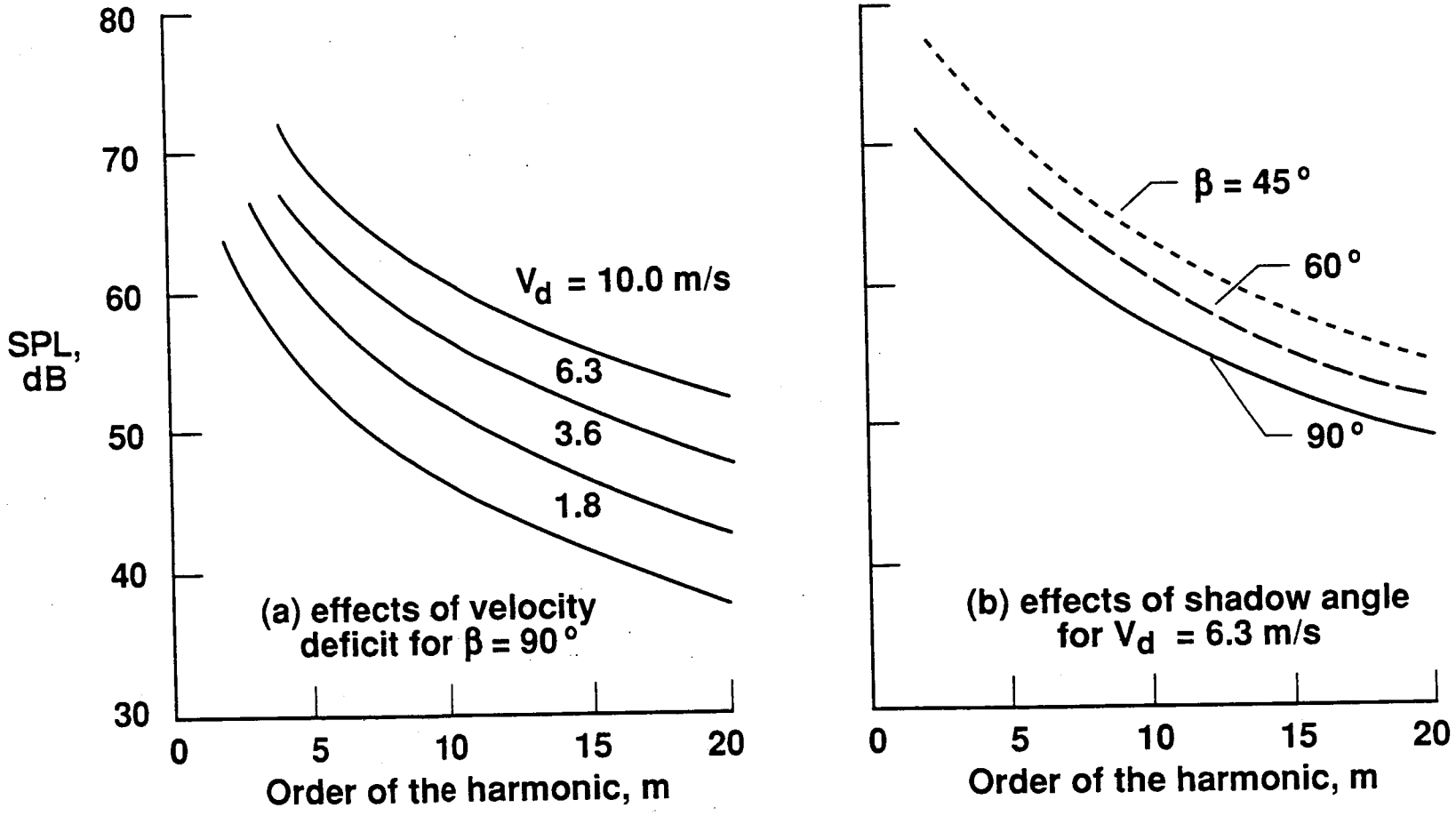

Figure 14. - Effects of wind speed deficit and shadow angle on the calculated rotational harmonic spectrum envelopes for the MOD5-B machine. P = 3000 kW, V = 12.5 m/s.

NASA

Report Documentation Page

1. Report No.	2. Government Accession No.	3. Recipient's Catalog No.
NASA TM-101567		

4. Title and Subtitle	5. Report Date
Environmental Noise Characteristics of the MOD5-B (3.2 MW) Wind Turbine Generator	March 1989
	6. Performing Organization Code

7. Author(s)	8. Performing Organization Report No.
Kevin P. Shepherd* and Harvey H. Hubbard**	
	10. Work Unit No. 535-03-11-03

9. Performing Organization Name and Address	11. Contract or Grant No.
NASA Langley Research Center Hampton, VA 23665-5225	
	13. Type of Report and Period Covered
12. Sponsoring Agency Name and Address National Aeronautics and Space Administration Washington, DC 20546	Technical Memorandum
	14. Sponsoring Agency Code

15. Supplementary Notes

*Langley Research Center, Hampton, Virginia.
**Planning Research Corporation, Hampton, Virginia.

16. Abstract

Both narrow band and broad band acoustic data were obtained for the MOD5-B wind turbine for a range of wind speeds from 5.8 to 14.3 m/s; for a range of power outputs from 300 to 3100 kW; and for various azimuth angles and distances. Comparisons are made with those of other large machines and with predictions by available methods.

The highest levels occur at the lower frequencies and generally decrease as the frequency increases. Low frequency rotational noise components were more intense than expected for an upwind machine and are believed to result from localized wind gradients across the rotor disk due to upwind terrain features. Predicted broad band spectra follow the general trends of the data but tend to under-estimate the levels in the frequency range where the turbulent boundary layer-trailing edge interaction noise is expected to be significant.

17. Key Words (Suggested by Author(s))	18. Distribution Statement
Wind Turbine Acoustics Noise Generation Noise Prediction Noise Measurement	Unclassified - Unlimited Subject Category 71

19. Security Classif. (of this report)	20. Security Classif. (of this page)	21. No. of pages	22. Price
Unclassified	Unclassified	28	A03